Nonintrusive Particle Motion Studies in the Near-Wall Region of a Pilot-Scale Circulating Fluidized Bed

Preetanshu Pandey and Richard Turton*

Chemical Engineering Department, West Virginia University, Morgantown, West Virginia 26506

Paul Yue and Lawrence Shadle

National Energy Technology Laboratory, Department of Energy, Morgantown, West Virginia 26507

A backscatter LDV system was used to record velocities of solid particles in the near-wall region of the riser section of a pilot-scale cold-flow CFB. The riser was 30.5 cm in diameter and 15.2 m in height. The bed material comprised cork particles with a Sauter mean diameter of 812 μm and a particle density of 189 kg/m^3. The superficial gas velocity was varied from 3.75 to 5.4 m/s with a solids circulation rate ranging from 3.4 to 17.1 kg/m^2·s. A bimodal velocity distribution was observed near the wall region. The mean velocity of solids was found to increase with increasing superficial gas velocity and decreasing solids circulation rate. The mean velocity of particles moving in the downward direction was relatively insensitive to changes in operating conditions. A criterion for defining clusters was proposed and justified, and the effects of operating conditions on the mean velocity and size of clusters were examined. The mean cluster velocity for most of the operating conditions was in the range of 0.8−1.4 m/s in the downward direction. The mean cluster size was found to increase with increasing solids-to-gas load ratio.

1. Introduction

1.1. Particle Velocity Measurements in Circulating Fluidized Beds. Circulating fluidized beds (CFBs) are used widely in many processes in the petroleum and chemical industries. They have been studied intensively in the past in efforts to improve such industrial processes as CFB combustion and gasification of coal and fluid-catalytic cracking (FCC). CFBs exhibit complex hydrodynamics, caused by interactions between the gas and solid phases.[1] Particle velocity is one of the key parameters in understanding such systems, as it affects the mixing; heat, mass, and momentum transfer; and erosion. Computational fluid dynamic models of gas−solids flow systems have been found to be inaccurate in describing flow dynamics in CFBs.[2,3] Simulations must accurately capture the particle interactions in the annular region to successfully capture the overall flow behavior. The individual particle velocity information can be used to estimate the turbulent intensity of the solid phase and to estimate the granular temperature. Information on the variation of particle velocity with the radial distance is important in establishing the shear rate or viscosity dependence of the gas−solids mixture on the granular temperature.

The major challenge in making velocity measurements is to maintain the flow characteristics during measurement. In general, this can be achieved completely either by utilizing a laser-based system in a nonintrusive mode of measurement or by imaging and particle-tracking techniques. A considerable amount of research has been done in the past to monitor the movement of solids in the CFB riser section. The various techniques used in the past are summarized in Table 1.[4−28] Techniques employed include optical and imaging methods, solids sampling, analysis of pressure and capacitance measurements, and the use of tracers. The use of fiber-optic probes is the most common, mainly because of the ease of operation and the ability to insert the probes into dense flow regimes and to measure the solids velocities across the entire radius or width of the CFB riser.[7,9−12,18,27,28] However, these methods are intrusive and risk potentially disturbing the flow field that is being studied. Additional optical methods include particle imaging techniques PIV[20] and stroboscopic analysis,[26] as well as laser fluorescence methods employing tracer species.[6,15] Another radioactive particle tracer study was used to characterize velocities in a large CFB.[22] The imaging techniques can be manpower-intensive in discriminating distinct particles and collecting sufficient points to characterize average behavior. The tracer techniques require either a strong radioactive source or the dilute flow regime to view the fluorescing particles. Pitot tube[5] and capacitance[13] probes use indirect measurements of solids velocities. Pitot tubes are prone to plugging, whereas electrical conducting materials and the buildup of charges or spurious electric fields hamper capacitance measurements. Extraction sampling probes have been used by several investigators,[8,14,19] but these are time-consuming, intrusive, cumbersome, and represent time-average responses over the relatively long sampling duration. Isokinetic sampling requirements are difficult to attain as a result of the nature of the fluctuating flow in CFBs, and the sampling data require additional information regarding the solids concentration to determine the solids velocity from the measured flux. Some of the other solids velocity measurement techniques, not tested directly in CFB risers, include image sensing,[29] video-imaging,[30] tracer studies,[31,32] strain gauge measurements,[33] radio waves,[34] electrostatic probes,[35] and acoustic measurements.[36]

Although laser Doppler velocimetry (LDV) measurements, both forward and backscatter, are limited to

* To whom correspondence should be addressed. Tel.: 304-293-2111 x2415. Fax: 304-293-4139. E-mail: riturton@mail.wvu.edu.

Table 1. Summary of the Measurement Techniques and CFB Operating Regimes Used by Various Researchers

		particle properties		operating conditions		CFB riser dimensions			
author(s)	bed material	ρ_p (kg/m^3)	d_p (μm)	M_s (kg/m^2·s)	U_g (m/s)	D (mm)	H (m)	fluidization regime(s)	particle movement monitoring technique
Arastoopour and Yang[4]	shale	2100	13	88, 133	2, 4.2	50.8	2.74	core−annulus dilute phase	LDA
Bader et al.[5]	FCC	1714	76	98−195	3.7−6.1	305	12.2	fast fluidization	Pitot tube
Hamdullahpur et al.[6]	sand	−	300	−	0.12−0.6	319 × 176	4	−	laser fluorescence
Hartge et al.[7]	FCC	1500	85	7−70	1.2−5.4	400	8.4	fast fluidization	fiber-optic probe
Herb et al.[8]	FCC sand	−	68, 125, 276	10−70	1−8	150	10.8	core−annulus dilute phase[a]	sampling probe
Herbert et al.[9]	FCC	1400	79	50−96	6.1	50[b]	4.7[b]	core−annulus dilute phase	fiber-optic probe
Horio et al.[10]	FCC	1000	60	11.2−11.8	1.2, 1.3	50	2.8	fast fluidization	fiber-optic probe
Issangya et al.,[11] Liu et al.[12]	FCC	1600	70	<550	4−8	76.2	6.1	dense suspension upflow and fast fluidization	fiber-optic probe
Louge et al.[13]	FCC	−	61	0−125	0.7−5	197	7	fast fluidization	capacitance probe
Miller and Gidaspow[14]	FCC	−	75	12−32.8	2.6−3.5	75	6.6	core−annulus dilute phase[a]	extraction probe
Morooka et al.[15]	silica gel	1250	1540	−	0.52−0.6	190	2.53	−	fluorescent tracer (measurement of fines)
Moortel et al.[16]	glass spheres	2400	120	solids vol fraction < 3%	0.8−1.2	200 × 200	2	core−annulus dilute phase	forward-scatter PDPA
Nieuwland et al.[17]	sand	2540	129	100−400	7.5−15	54	8	dense flow, fast fluidization	optical probe
Parssinen and Zhu[18]	FCC	1500	67	<550	<10	76	10	dense suspension upflow, fast fluidization	five-fiber optical probe
Rhodes et al.[19]	alumina	1800	64	42, 63	2.8, 4	150	5.4	fast fluidization	sampling probe
Shi et al.[20]	river sand	3020	382	1.5−2.75	2.8−4	200 × 200	4	fast fluidization	PIV
Tsuji et al.[21]	plastic	1020	200−3000	particle/air mass flow rate < 5	8−20	30	5.1	core−annulus dilute phase	forward-scatter LDV
Viitanen[22]	FCC	2400	70	289−488	7	1000	39	fast fluidization	radioactive tracking (measurement of fines)
Wang et al.[23]	FCC	1670, 1398	36, 54	1−70	1−7	140	10.4	core−annulus and homogeneous dilute phase	LDV
Wei et al.[24]	FCC	1398	54	18−200	2.3−6.2	186	8	core−annulus dilute phase and fast fluidization	modified backscatter LDV
Yang et al.[25]	FCC	1545	54	6−134	1.5−6.5	140	11	core−annulus and homogeneous dilute phase	backscatter LDV
Zheng et al.[26]	sand	4420, 3580	153, 270	60, 62	6.5, 4.2	152	9.3	fast fluidization	stroboscopic photography
Zhou et al.[27]	Ottawa sand	2640	213	20, 40	5.5−7	146 × 146	9.1	fast fluidization	five-fiber optical probe
Zhu et al.[28]	FCC	1500	67	49−208	3.7−10.2	100	−	core−annulus dilute phase and fast fluidization	five-fiber optical probe
this study	cork	189	812	3.4−17.1	3.75−5.4	305	15.2	fast fluidization	backscatter LDV

[a] Assuming particle density = 1500 kg/m^3. [b] Downer dimensions.

either near-wall or very dilute flows, their simplicity, accuracy, and capability of measuring individual particle velocities have resulted in their being selected as the method of choice by many CFB research groups.[4,16,21,23−25] LDV, the measurement technique used in this study, is an advanced nonintrusive optical technique for instantaneous local measurements of solid particle velocities and can provide insight into the turbulence intensity. All flow field characteristics are retained, and minimal calibration is required.[37] In general, two main problems are encountered in using LDV for dense solids flow measurements:[24] (1) Measurement is hampered by the simultaneous appearance of more than one particle in the measurement volume. (2) The intensity of the beam and its scattered light decays exponentially with the penetration distance into the dense gas−solids suspension, thereby affecting the signal.

For the solids material (cork) used in this study, the first problem is not an issue because the individual particle size is greater than the measurement volume. The second problem, however, remains a concern, and the relation between bed-penetration distances as a function of the solids loading is addressed in this study. However, LDV can still be used successfully to obtain valuable particle velocity information in the near-wall region, even for relatively dense conditions, without perturbing the flow.

The operating regimes of the fluidized beds of the various researchers were evaluated using the correlations proposed by Bi and Grace[38] and are included in Table 1. Data were collected over dilute, fast-fluidized, core−annulus, up-to-dense suspension upflow operating regimes. However, most of the studies were conducted to evaluate the velocity measurement technique in relatively small-diameter CFB risers. As a result, the data sets generated were dominated by wall effects rather than gas−solids hydrodynamics. As summarized in Table 1, only four of the studies, including this study, were conducted on CFB risers larger than 30 cm in diameter. In these studies, all of these tests were conducted with relatively dense bed material in the fast fluidization regime and the solids velocity measuring

techniques used included radioactive tracers,[22] Pitot tubes,[5] and fiber-optic probes.[7] Thus, detailed data obtained using the accurate and nonintrusive LDV method are lacking, particularly for particles near the wall region of large-diameter risers. Test data using larger particles and lighter bed materials permit easier isolation and detection of individual particles while minimizing the effects of gas expansion due to the pressure drop across the bed. In addition, the use of larger particles leads to lower number densities at a given mass flow rate and, hence, improves laser penetration into the bed.

1.2. Studies on "Clustering" Phenomena in the Near-Wall Region. The study of particle motion near the wall region (annular flow) is of particular interest in understanding the mechanism of heat transfer with the wall. This becomes especially important in cases where combustion temperatures are to be maintained as the boiler load varies.[39] The flow in a circulating fluidized bed is generally characterized by a rapidly rising and relatively dilute suspension in the core surrounded by a slow-falling, denser suspension (annulus) near the wall. The annulus is made up of alternating dilute-phase and dense-phase "clusters". The formation of clusters has been suggested to be one of the key factors for the high slip velocities observed in CFB risers.[39] Information on clusters can be very important for modeling heat and mass transfer, chemical reactions, and the hydrodynamics of CFB risers, as well as wall erosion.[40,41]

The measurements of cluster velocities made by various researchers have been summarized well by Harris et al.,[40] Glicksman,[42] and Griffith and Louge.[43] The kinds of measurement techniques used in previous studies to observe the clustering phenomenon are capacitance probes,[13,44,45] optical fiber probes,[7,10,27,46] extraction probes,[14] thermal imaging (TIV),[47] high-speed imaging,[39,41,48,49] particle impact probes,[50] γ-radiation,[51] laser sheet imaging,[52] and theoretical modeling.[53,54] The primary response variables examined in most of the previous studies are the cluster velocity, cluster length, and void fraction within a cluster. Typical cluster velocities are reported to lie between 0.2 and 3 m/s, with most of them close to 1 m/s.[40,44,48] Typical cluster sizes, reported by various researchers, lie in the relatively broad range of 0.22−47 mm.[40] The mean solids volume fractions within a cluster reportedly range anywhere from 0.002 to 0.48.[40] All three parameters are functions of the type of particles used in the study, the size and operating regime of the CFB, and the measurement location in the CFB riser. A correlation for cluster void fraction, mean cluster size, and mean cluster velocity, for a particular range of operating conditions, was suggested by Harris et al.[40] and seems to agree well with most of the previous studies. Sharma et al.[45] proposed a criterion to identify a cluster on the basis of the particle concentration. They concluded that the solids volume fraction in clusters was not dependent on particle size but decreased with increasing gas velocity. Moortel and Tadrist[55] suggested that the particle cluster sizes are strongly related to the local characteristics of the velocity field.

Griffith and Louge[43] presented a very simple correlation relating the cluster velocity (u_{cl}) and particle diameter (d_p) given by eq 1, which agrees reasonably well with the velocity measurements made by several researchers

$$u_{cl} = 36\sqrt{g d_p} \tag{1}$$

This equation appears to be remarkably robust, considering the broad variations in operating and experimental conditions. This correlation was modified by Noymer and Glicksman[47] to incorporate the effect of particle density and to provide even more generality

$$u_{cl} = 0.75\sqrt{\frac{\rho_p}{\rho_f} g d_p} \tag{2}$$

where ρ_p refers to the particle density and ρ_f to the fluid density.

Rhodes et al.[39] coined the term "swarms" for particles in contact with the wall that moved typically at 0.3−0.4 m/s. They also indicated that, a few millimeters away from the wall, there is a steady bulk downflow of particles, which they termed "particle strands", descending at approximately 1 m/s for suspension densities greater than 5.6 kg/m^3. Yerushalmi et al.[56] used terms such as "streamers", "strands", and "ribbons" to describe this group of particles. The main source of the variations in the results obtained by various researchers arises from the uncertainty in the definition of a cluster. One of the most comprehensive definitions of a cluster was proposed by Soong et al.[44] Lints and Glicksman[50] developed criteria on the basis of the experimental conditions and measurement technique (particle impact probe) they used. An important issue that remains to be fully resolved is whether these clusters exist in an industrial-scale unit. This study is a step toward addressing this issue by performing experiments and studying the clustering phenomenon near the wall region of a pilot-scale CFB riser.

2. Experimental Setup and Apparatus

The experimental test facility used in this study is a cold-flow circulating fluidized bed (CFB), located at the National Energy Technology Laboratory (NETL), U.S. Department of Energy, Morgantown, WV. This system has been described by Monazam et al.[57] A schematic diagram of this facility is shown in Figure 1. This unit is an atmospheric-pressure, cold-flow model of a CFB combustor. The riser is 30.5 cm in i.d. and 15.2 m in height with a standpipe i.d. of 25.4 cm. The riser is rigidly fixed to the building structural beams. Structural vibrations have been observed in the building due to the motion of solids in the standpipe during slip−stick flow or in the riser during turbulence or slugging; however, the air supply is obtained from compressors housed remotely, 75−100 m away, and the only vibrations observed from the gas supply are due to the high-frequency noise from the pressure letdown valve that is separated from the project by a large 3.05-m-diameter, 7.6-m-high air storage tank. The cork bed material is so light that pressure fluctuations and solids flow vibrations in the standpipe were easily eliminated using 0.254-m (10-in.) and 0.3048-m (12-in.) schedule 40 carbon steel components and 10.33 bar (150 lb) flanges. The optics bench was also rigidly mounted to the structural steel beams in the facility.

The CFB is instrumented with aeration flow control loops, differential pressure transmitters, load cells, and a spiral device,[58] developed at NETL, to measure the solids circulation rate. Solids are transported from the standpipe to the riser through a fully fluidized nonme-

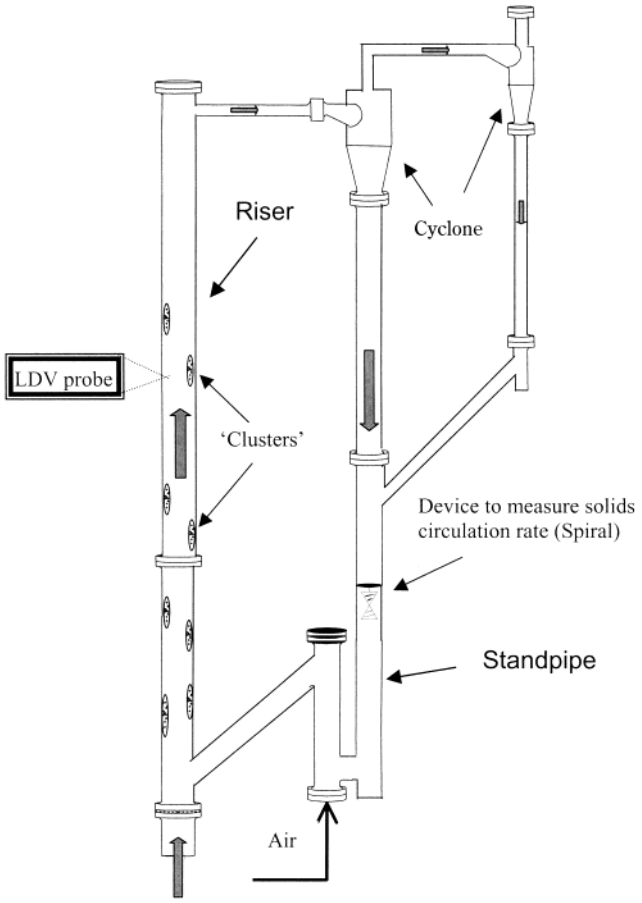

Figure 1. Schematic representation of the circulating fluidized bed setup at NETL, Department of Energy facility, Morgantown, WV.

chanical valve (loop-seal). Two staged cyclones capture the particles leaving the riser, which are then returned to the standpipe. The CFB walls are metallic, to prevent static buildup, with some sections made of acrylic (Plexiglas) to allow for visual observation and provide clear optical access to instruments, such as the LDV used in this study.

The LDV was set up to take velocity measurements at a height of 9 m from the bottom of the riser section. The LDV was placed on a platform supported by a linear slide to enable it to make velocity measurements at selected radial locations inside the riser section. The setup consists of a hand crank that rotates a drive screw, which, in turn, guides the movement of the slide. A precalibrated counter attached to the screw converts the screw rotation value to a linear distance with an accuracy of 10 μm. This setup enabled the accurate positioning of the measurement volume of the LDV within the bed.

3. Measurement Technique

The LDV system used in this study is a component of a TSI Backscatter Imaging LDV System (BILS).[37] In brief, BILS is a combination of an LDV and an imaging system and provides simultaneous velocity (using the LDV) and particle size (using a CCD camera) measurements. However, because of the high light attenuation and dispersion of the Plexiglas surface, sharp images of the particles could not be obtained in this study. Hence, no meaningful information on particle size could be derived. The effect of plexiglass on the velocity measurements in the z (axial) direction was studied independently and found to be insignificant.[37] The LDV component can work independently of the imaging system and was used successfully to provide axial velocity measurements in this study.

The LDV unit of BILS is different from a conventional LDV in the sense that it has both of the probes (transmitter and receiver) combined into one transceiver unit. Thus, it works in the backscatter mode and requires only one optical window to access the flow. Also, maintaining optical alignment between two separate probes, which is normally a problem for LDVs operating in a forward scattering mode, is automatic. An air-cooled argon ion laser with 750-mW peak output power serves as the light source. The laser beam passes through a fiber drive where a Bragg cell is used to split it into two beams of equal intensity. An interference pattern, characterized by a set of dark and bright fringes, can be observed at the intersection point of the two beams. The plane of the interference pattern lies along the bisector of the two beams. As a particle crosses these fringes, Doppler light pulses are generated that are scattered back to the transceiver. After real-time processing of the signal, the results are displayed on the computer by DataView NT software. The components of the system are shown in Figure 2.

The velocity is calculated using the equation

$$V = dF_{\mathrm{D}} \tag{3}$$

where F_{D} is the Doppler frequency, V is the particle velocity, and d is the fringe spacing, which is given by

$$d = \frac{\lambda}{2\,\sin(\beta/2)} \tag{4}$$

where λ is the wavelength of the laser beam and β is the beam-crossing angle.

In a turbulent system, such as a CFB, it is important to distinguish between the upflow and downflow of particles, as the local velocity can change direction. This is achieved by a Bragg cell that shifts the frequency of one of the beams, resulting in a moving pattern of fringes, which permits an unambiguous determination of the direction of motion. The validation and initial testing of this unit were conducted by measuring terminal velocities of near-spherical Nu-Pareil sugar particles of different sizes and comparing them with predictions from terminal velocity correlations proposed by Haider and Levenspiel.[59] The results were found to be in good agreement.[37]

4. CFB Material

The solids phase consisted of 812-μm (Sauter mean diameter) cork particles. Cork, when tested at ambient conditions in air, has a solid/gas density ratio similar to that of coal and combustion gas at 10−20 atm and 1000 ° C.[60] Therefore, it is an excellent material to generate data relevant to advanced, high-pressure, coal conversion processes. The particle size distribution of the cork material used is shown in Figure 3. Its bulk density is in the range of 88−107 kg/m^3, with a particle density of 189 kg/m^3 and a sphericity estimated to be 0.84. Solids volume fractions under vibrated and fluffed conditions were measured as 0.515 and 0.423, respectively. The minimum fluidization velocity is 0.07 m/s. The terminal velocity of the material was measured

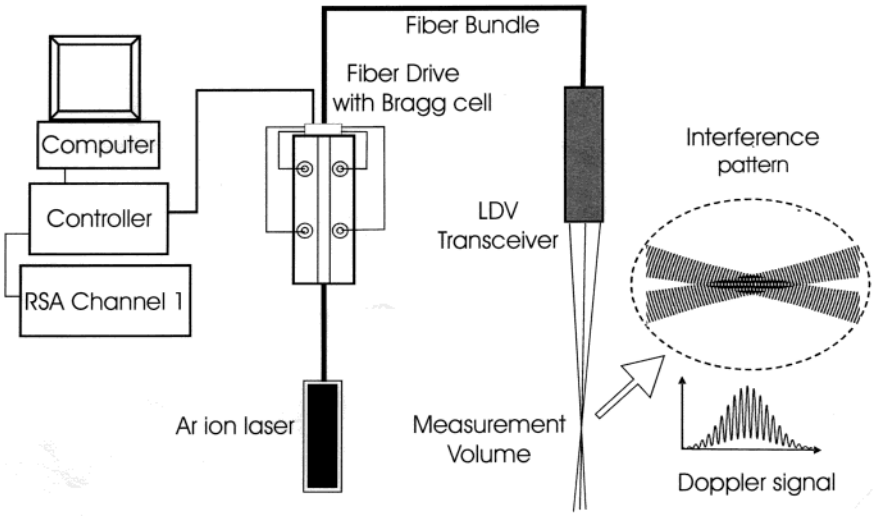

Figure 2. Main components of the TSI backscatter LDV system used for 1-D solids velocity measurements.

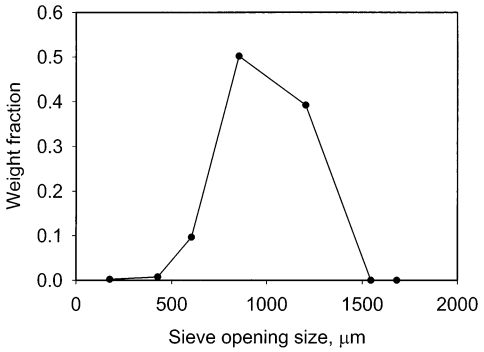

Figure 3. Particle size distribution of the cork material with a mean Sauter diameter of 812 μm.

Table 2. Mean Terminal Velocities of Different Particle Sizes Cuts of Cork Material

size (μm)	mean terminal velocity (m/s)
700−850	0.86
850−1000	0.95
1000−1200	1.38

using the LDV for three particle size cuts and is reported in Table 2.

5. Results and Discussion

A fully randomized and replicated statistically designed experimental matrix was used to ensure that a wide range of operating conditions in the fast-fluidized regime was covered, including examples of dilute (fluid-dominated[61]), core−annulus, and dense suspension (particle−fluid compromising[61]) cases.[60] These tests were conducted at velocities above which an S-shaped axial pressure profile could be found. The tests were conducted using a central composite design with two independent variables, namely, the riser superficial gas velocity, U_g, and the solids circulation rate, M_s. Each variable was tested over five levels. The center point in the matrix (M_s = 2722 kg/h, U_g = 4.58 m/s) was duplicated within each replicate set to ensure that there was no time variation due to uncontrolled parameters. All measurements were taken at steady-state conditions and at atmospheric pressure and temperature. The temperature and pressure at the base of the riser were controlled to 21 °C and 1.062 bar, respectively. This

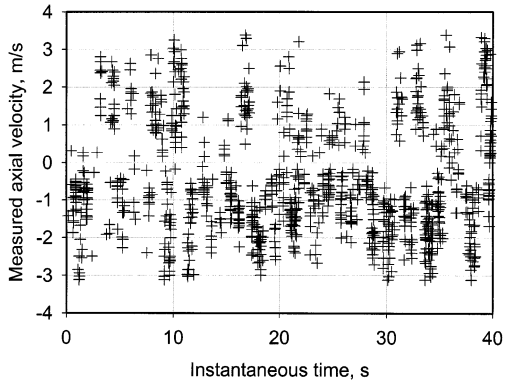

Figure 4. Typical temporal evolution of a particle's axial velocity obtained 1 mm from the wall of the riser section of the CFB at a location of z = 9 m from the bottom (negative velocity indicates that the particle is moving downward).

produced a constant gas density of 1.248 kg/m^3 at the base of the riser. The temperature was controlled using a process air heat exchanger with a PID feedback control system adjusting the flow of water to the shell-and-tube heat exchanger. Hot or cold water was used to control the air temperature depending on whether the air temperature was too cold or too hot, respectively. The pressure was controlled using a back-pressure control valve and a PID controller to drive the valve. The pressure transmitter used for the feedback was located at a distance of 7.6 cm above the distributor.

Several trial runs were conducted to ensure that the instrument gave repeatable results.[37] The typical time for which data were recorded for measurements near the wall generally varied from 30 to 45 s. Such a data set contained a little over 1000 data points. The acquisition time was chosen individually for all operating conditions to ensure that a sufficient number of measurements for statistical analysis were acquired.

A typical velocity versus time graph, obtained 1 mm from the wall, during a run with M_s = 2722 kg/h and U_g = 4.58 m/s, is shown in Figure 4. Instantaneous velocity data for each solid particle passing through the measurement volume were recorded with time. A negative velocity on the graph indicates that the particle was moving in the downward direction. The frequency distribution of velocities during a run under the same conditions (M_s = 2722 kg/h, U_g = 4.58 m/s) is shown in Figure 5. Near the wall, a greater number of particles

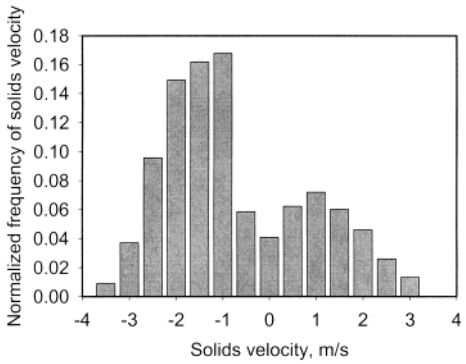

Figure 5. Typical velocity distribution obtained 1 mm from the wall of the CFB riser at a location $z = 9$ m location from the bottom showing bimodal distribution of velocity.

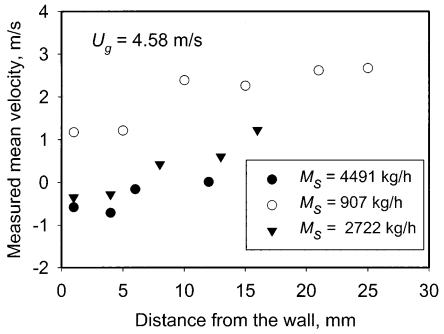

Figure 6. Effect of the solids circulation rate on the mean velocity near the wall region at a location $z = 9$ m from the bottom for a superficial gas velocity of $U_g = 4.58$ m/s: $M_s = 907$, 2722, and 4491 kg/h.

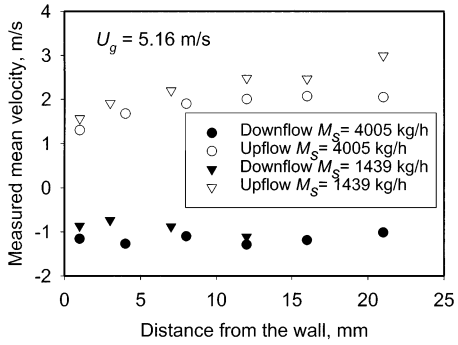

Figure 7. Effects of solids circulation rate on upflow and downflow of solids near the wall region for $U_g = 5.16$ m/s: $M_s = 4005$ and 1439 kg/h.

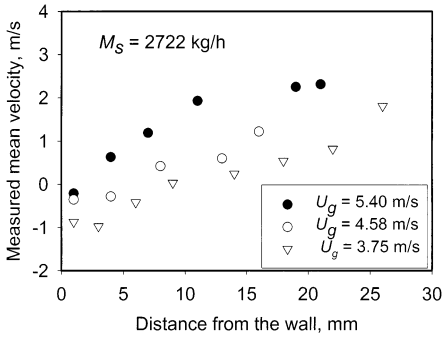

Figure 8. Effect of superficial gas velocity on the mean velocity near the wall region at a location $z = 9$ m location from the bottom for a solids circulation rate of $M_s = 2722$ kg/h: $U_g = 5.4$, 4.58, and 3.75 m/s.

moved in the downward rather than upward direction. It should also be noted that the distribution was bimodal. For this reason, it was decided to study the upward and the downward flows separately, in addition to the net flow of solids. It was also evident from the results presented in Figure 4 that most of the particles moving downward had velocities in the range of 1−2 m/s.

5.1. Effects of Solids Circulation Rate. The experimental matrix allowed the separate study of the effects of solids circulation rate and superficial gas velocity on the flow behavior in the CFB riser. The effect of the solids circulation rate on the solids velocity profile is shown in Figure 6, where the superficial gas velocity was kept constant at 4.58 m/s. It was observed that the mean velocity of solids shifted toward the negative direction with increasing circulation rates, indicating that more of the solids near the wall were moving downward. This is consistent with the core−annulus flow pattern expected in a riser and was confirmed by visual observation. The frequency of particles (solids) being detected near the wall was found to increase with increasing solids circulation rate. In addition, a greater fraction of solids were found to move downward. The mean velocity of solids was found to decrease with increasing solids circulation rate at this near-wall location. This is consistent with the results reported by Wei et al.[24] and Yang et al.[25] At a very high solids circulation rate ($M_s = 4491$ kg/h), almost all particles appeared to be moving downward near the wall region. For the most dilute condition in this study, $U_g = 4.58$ m/s, $M_s = 907$ kg/h, the net flow of solids everywhere in the riser was upward; thus, the core−annulus type of flow was not observed for this case at that axial measurement location. However, even for this case, measurements over the entire cross section were not possible because of particles obstructing the path of the laser beam.

A similar analysis was carried out at two different superficial gas velocities for two different solids circulation rates ($M_s = 4005$ and 1439 kg/h, at $U_g = 5.16$ and 3.75 m/s). The results for the higher velocity are plotted in Figure 7. The mean velocities of the particles moving upward and downward were examined separately. At 1 mm from the wall, it was observed that the upward solids velocity decreased and the downward solids velocity increased with increasing solids circulation rate. This observation is consistent with the results obtained by Tadrist and Cattiuw,[62] Yang et al.,[25] and Zhou et al.[27] These results were attributed to the fact that an increase in the solids circulation rate caused the gas velocity near the walls to decrease.

It was also observed that the negative velocity was relatively insensitive to the changes in solids circulation rate. As the solids flow rate increased, the number of particles moving downward near the wall increased, but the mean downward velocity did not change. This averaged downward velocity was also remarkably invariant with radial location. Again, the number of particles contributing to the average downward flow was generally lower as the radial position was moved away from the wall, but the particle velocity remained unchanged at about 1 m/s.

5.2. Effects of Superficial Gas Velocity. To study the effects of the superficial gas velocity on the solids velocity profile near the wall, a constant solids circulation rate was maintained. The velocity profiles for three superficial gas velocities ($U_g = 5.4$, 4.58, and 3.75 m/s) are shown in Figure 8 for a constant solids circulation rate of $M_s = 2722$ kg/h. The mean velocity increased

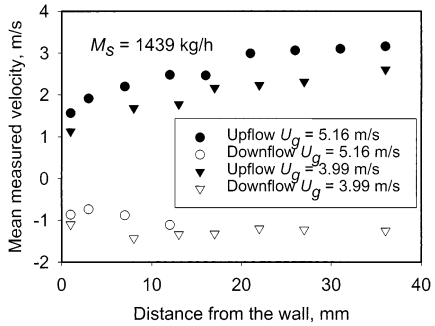

Figure 9. Effect of superficial gas velocity on the mean velocity near the wall region for a solids circulation rate of M_s= 1439 kg/h: U_g = 5.16 and 3.99 m/s.

with increasing superficial gas velocity. This trend is consistent with the results reported by Moortel et al.[16] and Nieuwland et al.[17] For all three conditions, the mean solids velocity was downward very close to the wall. Similar test cases were considered at a different solids circulation rate for two different superficial gas velocities. The results are shown in Figure 9. As expected, the velocities of the upward-moving particles increased with increasing superficial gas velocity. The number of particles moving downward was found to decrease with increasing superficial gas velocity. These results are in agreement with those reported by Yang et al.[25] and Zhou et al.[27] Again, it was observed that the mean velocity of downward-moving particles was relatively insensitive to the change in superficial gas velocity. This has also been reported by Zhou et al.,[27] who varied the gas velocity over a range of 5.5−7 m/s. Similarly to the effect of solids circulation rate, the superficial gas velocity did not influence the mean downward flowing velocity. Furthermore, the radial position had no discernible impact on the mean negative velocity.

A statistical analysis [ANOVA test, significance (α) = 0.05] was carried out on the complete composite test matrix to estimate the significance of the operating variables (U_g and M_s) on the mean velocity of solids at the wall. A significant effect was measured for both U_g (α = 0.014) and M_s (α = 0.005), but the interaction between U_g and M_s was found to be insignificant (α = 0.18). Furthermore, the test revealed that the solids velocity was affected more by changes in the superficial gas velocity than in the solids circulation rate. A similar effect was also observed in past experiments by Nieuwland et al.[17] and Karri and Knowlton.[63]

6. Cluster Formation

Because of the wealth of data collected over various operating conditions, this study contained much useful information on the formation of clusters near the walls of the riser. As seen in Figure 4, many successive signals occurred over short time intervals; these time-correlated signals were probably due to the passing of clusters. One of the most challenging tasks in any study on clusters is to define what constitutes a cluster. Criteria for defining clusters are proposed and discussed in detail in the following section. The effects of the operating conditions on the velocity and size of clusters are also examined.

6.1. Cluster Definition. A cluster can be defined as a group of particles that moves together with a certain voidage in order to minimize the drag acting on it. Thus, the velocities of the individual particles constituting a cluster are fairly close to each other, even though the cluster might, in itself, be accelerating or decelerating. In addition, the particles comprising the cluster will pass through a particular location in space (the measurement volume in this study) within a certain period of time. This time period will depend on the cluster velocity, the void fraction of particles within the cluster, and the size of the cluster. Lints and Glicksman[50] used a particle impact probe to study clusters and defined a cluster as a group of five or more sequential particle strikes with some maximum allowable time between any two sequential strikes. They suggested that this time to be either 2 or 4 ms for the particles used in their study, which were 182 μm in diameter.

In the present work, a cluster was identified when all of the following conditions were met: (1) The difference in time between any two successive particle measurements was greater than t_{same}, to account for multiple hits by the same particle. (2) The difference in time between two successive particle measurements was less than t_{diff}. (3) At least four sequential particle hits satisfied the other three criteria (n_{hits}). (4) The velocity difference (v_{diff}) between any particles in a cluster was within $\pm$1 m/s of the mean velocity of the other particles of that cluster.

A Visual Basic code was written to separate clusters from the raw data and study them independently. With this code, the parameters in the above criteria were varied, and the effect of each one was analyzed separately. To estimate the values of t_{same}, the time taken by a particle to pass through the measurement volume was used. A particle, on average, has to travel a distance of 30 μm to cross the measurement volume. Thus, the time within which the same particle can produce another Doppler burst can be estimated by the equation

$$t_{same} = \frac{\delta\ (\mathrm{m})}{v\ (\mathrm{m/s})} \tag{5}$$

where v is the velocity of the individual particle in meters per second and δ is the relevant length, in meters, of the sample volume. Any two or more sequential particle hits recorded within this time limit were considered to be the same particle and discarded from the analysis of clusters. The velocity difference criterion is based on the fact that the particles within the same cluster will move at fairly similar velocities. The value of 4 for n_{hits} was based on the results of previous researchers.[45,50] One of the reasons n_{hits} is lower than the value suggested by Lints and Glicksman[50] is that the measurement volume in this study is much smaller and, hence, fewer cluster particles are expected to pass through it in a given time frame. A sensitivity analysis showed that, although the choice of t_{diff} had a significant influence on the cluster characteristics (especially cluster size and velocity), these characteristics were not greatly affected by the choice of t_{same}, v_{diff}, and n_{hits} around the values chosen.

It was observed that the parameter having the greatest effect on the cluster properties was t_{diff}. To obtain an initial upper estimate of t_{diff}, it was assumed that the particles in a cluster are symmetrically placed on the edges of a cube. The distance between them is then given by

$$\text{distance between particles} = d_p \sqrt[3]{\frac{\pi}{6(1-\epsilon_c)}} \quad (6)$$

where d_p is the particle diameter and ϵ_c is the cluster voidage. The cluster voidage (ϵ_c) was evaluated using the correlation suggested by Lints[64] (eq 7). The pressure balance across the riser was used to estimate the voidage in the dilute phase (ϵ) for different operating conditions and is given by eq 8

$$\epsilon_c = 1.23(1-\epsilon)^{0.54} \quad (7)$$

$$\frac{\Delta p}{L} = \rho_p g(1-\epsilon) \quad (8)$$

where Δp is the pressure drop, ρ_p is the particle density, and L is the length of the riser. The Sauter mean diameter of 812 μm was used to estimate the distance between particles in eqs 6−8. Finally, to estimate the upper limit of t_{diff}, the velocity of the most slowly moving particle (∼0.1 m/s) was used, with t_{diff} = distance/velocity. The calculated values for the upper limit of t_{diff} ranged between 13 and 15 ms. The value of t_{diff} was varied from 1 to 19 ms, and its effect on the predicted number of clusters is illustrated in Figure 10 for three sets of operating conditions. All of the runs shown were conducted over a time span of 30 s. As t_{diff} was increased from 1 ms, the estimated number of clusters increased. The effect of t_{diff} leveled off for all conditions at a value close to 12 ms, and this value of t_{diff} was then used in the subsequent analysis. For the most dilute conditions, the leveling effect was observed at a lower t_{diff} value (9 ms). However, the cluster characteristics were found to change minimally as t_{diff} was changed from 9 to 12 ms for the dilute case. An increase in the number of clusters for very high t_{diff} values (>16 ms) is explained by the fact that the software starts to predict clusters comprising individual particles spaced far apart. As expected, around the 12-ms mark, the densest case (M_s = 4491 kg/h, U_g = 4.98 m/s) was seen to have the maximum number of clusters. The cluster frequency was found to lie in the range of 1.4−3 Hz, as shown in Figure 11, and was found to increase with increasing solids-to-gas load ratio, defined by eq 9 below. Sharma et al.[45] reported that the cluster frequency lies between 6 and 11 Hz and also found that it decreases with increasing particle size for the two particle sizes (70 and 120 μm) that they used. The results here are consistent with this result, in that lower cluster frequencies were obtained for the much larger particles used in this study.

Using the above cluster criteria, the mean velocity and size of the clusters moving in the downward direction were estimated and used to study the effects of the operating parameters. The cluster size was obtained by taking the product of the length of time taken by a cluster to pass through the measurement volume and its mean velocity. Because the technique used here essentially measures the intersected chord length of the cluster, the actual cluster size is somewhat greater (on the order of 2 cm). A dimensionless solids-to-gas load ratio (m) was defined to characterize the operating conditions. This is given by eq 9, where A is the cross-sectional area of the riser

$$m = \frac{M_s}{\rho_f A U_g} \quad (9)$$

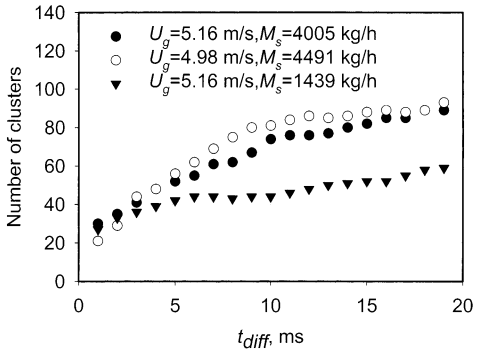

Figure 10. Effect of maximum allowable time between consecutive hits (t_{diff}) on the number of clusters for three operating conditions.

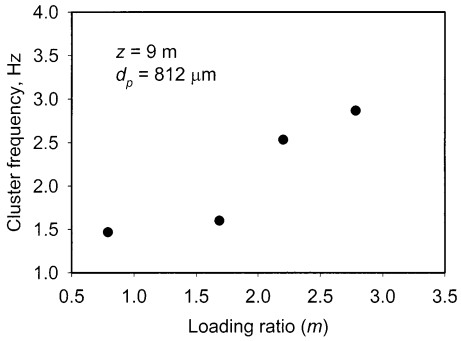

Figure 11. Variation of cluster frequency with dimensionless solids-to-gas load ratio.

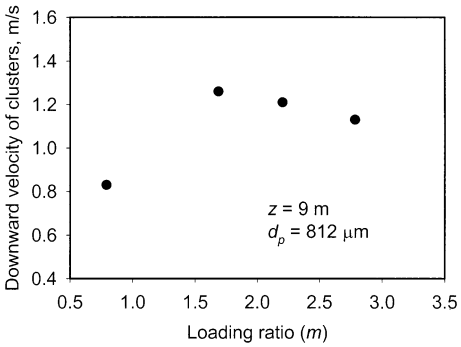

Figure 12. Variation of mean cluster velocity with dimensionless solids-to-gas load ratio.

The velocity of clusters moving downward was found to be in the range of 0.8−1.4 m/s, as shown in Figure 12. Subsequent analysis showed that the velocity of clusters moving downward was independent of the operating conditions. The cluster velocity predicted by eq 2 was 0.83 m/s, which was fairly close to the results obtained for most of the operating conditions. Equation 2 agreed very well for the case with the lowest loading ratio but underpredicted the results for the higher loadings. The velocity distribution of the clusters for a loading ratio of 2.83 is shown in Figure 13. Most of the clusters are seen to be moving at a velocity of 1−2 m/s.

The mean cluster size was found to be in the range of 0.6−1.8 cm. The relatively low values of cluster size, in comparison with those predicted by Soong et al.,[44] might be due to the tortuous path of the cluster passing the measurement volume. Thus, only an intersected chord length is measured, which will be smaller than the maximum length scale of the cluster. This is in agreement with the works of Noymer and Glicksman,[47] Lim et al.,[49] and Wu et al.[65] The mean cluster size was

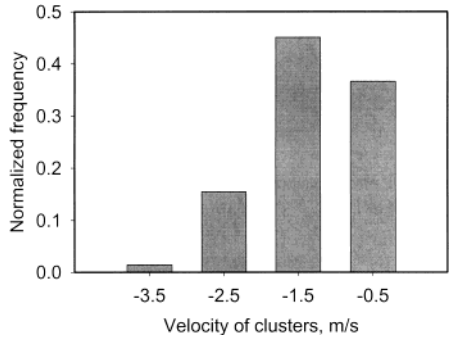

Figure 13. Distribution of cluster velocity at a solid-to-gas load ratio of 2.83.

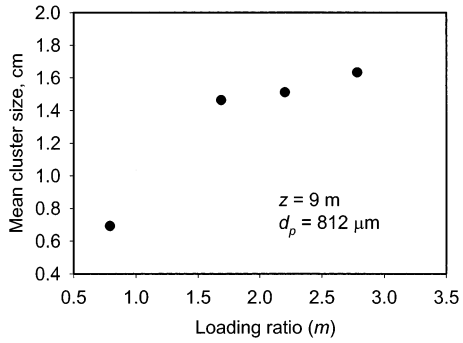

Figure 14. Variation of mean cluster size with dimensionless solids-to-gas load ratio.

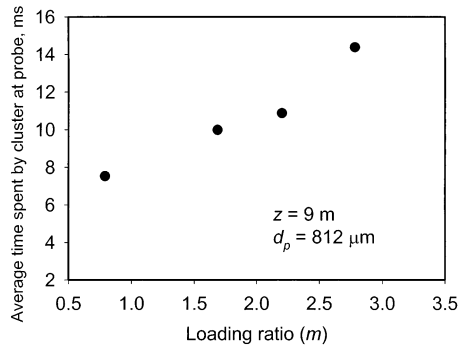

Figure 15. Variation of mean cluster time required by a cluster to pass through the measurement volume.

found to increase with increasing loading ratio and is shown in Figure 14. Thus, larger clusters were observed for denser conditions. The average time (number-average) taken by a cluster to pass through the measurement volume was estimated and plotted as a function of the solids loading. This is shown in Figure 15 and is seen to exhibit an increasing trend with loading ratio.

7. Conclusions

For the operating conditions used in this study on cork particles, the mean solids velocity was found to increase with increasing superficial gas velocity and decreasing solids circulation rate. The mean velocity was influenced more by the superficial gas velocity than by the solids circulation rate. A bimodal distribution was observed near the wall region. The velocity of downward-moving particles was found to be fairly constant and insensitive to changing operating conditions and sampling location.

Using the proposed criteria to define a cluster, it was found that the velocity of clusters moving downward was in the range of 0.8−1.4 m/s but followed no definite trend with increasing load ratio. Most of the clusters were found to be moving at a velocity of 1−2 m/s. The cluster frequency was found to be in the range of 1.4−3 Hz and was found to increase with increasing loading ratio. Finally, the mean cluster size was found to increase with increasing loading ratio.

The riser velocity profiles and cluster frequencies and velocities provide compelling evidence for mechanisms for wide variations in gas−solids mixing in a riser operated in the dilute-to-core−annulus flow regime. Under the more dilute flow conditions identified by low load ratios, the solids velocity was found to be upward at all radial positions; however, even at these conditions, clusters form at the wall and fall at the characteristic velocity for the bed material, creating a localized eddy. As the solids loading ratio increases, the number of clusters or the frequency of clusters grows, involving a larger cross section of the flow field. As a result, the upward flow is compressed into a smaller area, resulting in higher velocities for the gas and solids mixtures flowing upward. This is the dominant feature in the regime identified by Li as particle−fluid compromising (PFC),[61] although it was not considered to be important with more dilute flows that were identified as fluid-dominated (FD).[61] Nevertheless, it is apparent that, even under dilute upflow conditions, clusters can be observed near the wall that can influence the overall flow profiles. For these reasons, computational fluid dynamics (CFD) models, even in this core−annulus flow regime, that use a Lagrangian description of the particles, assuming that they are point masses (i.e., have no volume) and do not interact with each other (i.e., experience no granular stress), are inadequate for risers. The Eulerian representation of the particles (or the more detailed discrete element model) still seems appropriate, where the size and interactions of the particles are tracked.

Acknowledgment

Support for this study by the University/NETL student partnership program, through National Energy Technology Laboratory (NETL), Department of Energy, is gratefully acknowledged. The authors are grateful to Dr. Joseph Shakal from TSI Inc. for his invaluable technical help with the instrument.

Nomenclature

A = cross-sectional area of the riser (m^2)
d_p = particle diameter (m)
D = riser diameter (m)
H = height of the riser section (m)
L = length of the riser (m)
m = dimensionless solids-to-gas load ratio
M_s = solids circulation rate (kg/h)
n_{hits} = minimum number of consecutive hits
t_{diff} = maximum allowable time difference between consecutive hits (s)
t_{same} = minimum time difference between two consecutive hits (s)
U_g = superficial gas velocity (m/s)
v_{diff} = maximum allowable velocity difference (m/s)
v = individual particle velocity (m/s)

Greek Letters

α = significance level in ANOVA
β = beam-crossing angle in eq 4
δ = length of the sampling volume in the z direction (m)

ϵ = voidage across the riser
ϵ_c = cluster voidage
Δp = pressure drop across the riser (Pa)
ρ_f = fluid density (kg/m^3)
ρ_p = particle density (kg/m^3)

Acronyms

ANOVA = analysis of variance
BILS = backscatter imaging LDV system
CFB = circulating fluidized bed
FCC = fluidized catalytic cracking
LDV = laser Doppler velocimetry
LDA = laser Doppler anemometry
NETL = National Energy Technology Laboratories
PIV = particle imaging velocimetry
TIV = thermal imaging velocimetry

Literature Cited

(1) Werther, J.; Hirschberg, B. In *Circulating Fluidized Beds*; Grace, J., Avidan, A., Knowlton, T., Eds.; Blackie Academic and Professional: London, 1997; pp 119−146.

(2) Knowlton, T.; Karri, S. Results of CFB Riser Modeling Challenge Problem 2. Presented at Session 197: Industrial Applications of Circulating Fluidized Beds, AIChE Annual Meeting, Reno, NV, Nov 4−9, 2001.

(3) Gidaspow, D. *Multiphase Flow and Fluidization: Continuum and Kinetic Theory Descriptions*; Academic Press: New York, 1994.

(4) Arastoopour, H.; Yang, Y. Experimental Studies on Dilute Gas and Cohesive Particles Flow Behavior Using a Laser Doppler Anemometer. In *Fluidization VII*; Potter, O. E., Nicklin, D. J., Eds.; Engineering Foundation: New York, 1991; pp 723−730.

(5) Bader, R.; Findley, J.; Knowlton, T. Gas/solids flow patterns in a 30.5-cm-diameter circulating fluidized bed. In *Circulating Fluidized Bed Technology II*; Basu, P., Large, J., Eds.; Pergamon Press: Oxford, U.K., 1988; pp 123−137.

(6) Hamdullahpur, F.; Pegg, M.; MacKay, G. A laser-fluorescence technique for turbulent two-phase flow measurements. *Int. J. Multiphase Flow* **1987**, *13*, 379−385.

(7) Hartge, E.; Rensner, D.; Werther, J. Solids concentration and velocity patterns in circulating fluidized beds. In *Circulating Fluidized Bed Technology II*; Basu, P., Large, J., Eds.; Pergamon Press: Oxford, U.K., 1988; pp 165−180.

(8) Herb, B.; Dou, S.; Tuzla, K.; Chen, J. Solids mass fluxes in circulating fluidized beds. *Powder Technol.* **1992**, *70*, 197−205.

(9) Herbert, P.; Gauthier, T.; Briens, C.; Bergougnou, M. Application of fiber optic reflection probes to the measurement of local particle velocity and concentration in gas−solid flow. *Powder Technol.* **1994**, *80*, 243−252.

(10) Horio, M.; Morishita, K.; Tachibana, O.; Murata, N. Solid distribution and movement in circulating fluidized beds. In *Circulating Fluidized Bed Technology II*; Basu, P., Large, J., Eds.; Pergamon Press: Oxford, U.K., 1988; pp 147−154.

(11) Issangya, A.; Grace, J.; Bai, D.; Zhu, J. Further measurements of flow dynamics in a high-density circulating fluidized bed riser. *Powder Technol.* **2000**, *111*, 104−113.

(12) Liu, J.; Grace, J.; Bi, H. Radial distribution of local particle velocity in a high-density circulating fluidized bed riser. In *Circulating Fluidized Bed Technology VII*; Grace, J., Zhu, J., de Lasa, H., Eds.; Canadian Society of Chemical Engineering: Ontario, Canada, 2002; pp 341−348.

(13) Louge, M.; Lischer, D.; Chang, H. Measurements of voidage near wall of a circulating fluidized bed riser. *Powder Technol.* **1990**, *62*, 269−276.

(14) Miller, A.; Gidaspow, D. Dense, Vertical Gas−Solid Flow in a Pipe. *AIChE J.* **1992**, *38*, 1801−1815.

(15) Morooka, S.; Kusakabe, K.; Ohnishi, N.; Gujima, F.; Matsuyama, H. Measurement of local fines movement in a fluidized bed of coarse particles by a fluorescent tracer technique. *Powder Technol.* **1989**, *58*, 271−277.

(16) Moortel, T.; Azario, E.; Santini, R.; Tadrist, L. Experimental analysis of the gas-particle flow in a circulating fluidized bed using a phase Doppler particle analyzer. *Chem. Eng. Sci.* **1998**, *53* (10), 1883−1899.

(17) Nieuwland, J.; Meijer, R.; Kuipers, J.; Swaaij, V. Measurements of solids concentration and axial solids velocity in a gas−solid two-phase flows. *Powder Technol.* **1996**, *87*, 127−139.

(18) Parssinen, J.; Zhu, J. Particle velocity and flow development in a long and high-flux circulating fluidized bed riser. *Chem. Eng. Sci.* **2001**, *56*, 5295−5303.

(19) Rhodes, M.; Laussmann, P.; Villain, F.; Geldart, D. Measurement of radial and axial solids flux variations in the riser of a circulating fluidized bed. In *Circulating Fluidized Bed Technology II*; Basu, P., Large, J., Eds.; Pergamon Press: Oxford, U.K., 1988; pp 155−164.

(20) Shi, H.; Wang, Q.; Wang, C.; Luo, Z.; Ni, M.; Cen, K. PIV measurement of the gas−solid flow pattern in a CFB riser. In *Circulating Fluidized Bed Technology VII*; Grace, J., Zhu, J., de Lasa, H., Eds.; Canadian Society of Chemical Engineering: Ontario, Canada, 2002; pp 161−168.

(21) Tsuji, Y.; Morikawa, Y.; Shiomi, H. LDV measurements of an air−solid two-phase flow in a vertical pipe. *J. Fluid. Mech.* **1984**, *139*, 417−434.

(22) Viitanen, P. Tracer studies on a riser reactor of a fluidized catalyst cracking plant. *Ind. Eng. Chem. Res.* **1993**, *32*, 577−583.

(23) Wang, Y.; Wei, F.; Wang, Z.; Jin, Y.; Yu, Z. Radial profiles of solids concentration and velocity in a very fine particle (36 μm) riser. *Powder Technol.* **1998**, *96*, 262−266.

(24) Wei, F.; Lin, H.; Cheng, Y.; Wang, Z.; Jin, Y. Profiles of particle velocity and solids fraction in a high-density riser. *Powder Technol.* **1998**, *100*, 183−189.

(25) Yang, Y.; Jin, Y.; Yu, Z.; Zhu, J.; Bi, H. Local slip behavior in the circulating fluidized bed. *AIChE Symp. Ser.* **1993**, *89* (296), 81−90.

(26) Zheng, Z.; Zhu, J.; Grace, J.; Lim, C.; Brereton, C. Particle motion in circulating fluidized beds via microcomputer-controlled color-stroboscopic photography. In *Fluidization VII*; Potter, O. E., Nicklin, D. J., Eds.; Engineering Foundation: New York, 1992; pp 781−789.

(27) Zhou, J.; Grace, J.; Lim, C.; Brereton, C. Particle velocity profiles in a circulating fluidized bed riser of square cross-section. *Chem. Eng. Sci.* **1995**, *50* (2), 237−244.

(28) Zhu, J.; Li, G.; Qin, S.; Li, F.; Zhang, H.; Yang, Y. Direct measurements of particle velocities in gas−solids suspension flow using a novel five-fiber optical probe. *Powder Technol.* **2001**, *115*, 184−192.

(29) Kamiwano, M.; Saito, F. Measurement method of flow velocity of liquid and irregular solid particles using an image sensor with an image fiber. *AIChE Symp. Ser.* **1984**, *80* (241), 122−128.

(30) Saadevandi, B.; Turton, R. The application of computer-based imaging to the measurements of particle velocity and voidage profiles in a fluidized bed. *Powder Technol.* **1998**, *98*, 183−189.

(31) Mann, U.; Crosby, E. Cycle time distribution in circulating systems. *Chem. Eng. Sci.* **1973**, *28*, 623−627.

(32) Raso, G.; Tirabasso, G.; Donsi, G. An impact probe for local analysis of gas−solid flows. *Powder Technol.* **1983**, *34*, 151−159.

(33) Lin, J.; Chen, M.; Chao, B. A novel radioactive particle tracking facility for measurement of solids motion in gas fluidized beds. *AIChE J.* **1985**, *31* (3), 465−473.

(34) Merry, D.; Davidson, J. 'Gulf stream' Circulation in Shallow Fluidized Beds. *Trans. Inst. Chem. Eng.* **1973**, *51*, 381−368.

(35) Klinzing, G.; Zaltash, Z.; Myler, C. Particle velocity measurements through electrostatic field fluctuations using external probes. *Part. Sci. Technol.* **1987**, *5*, 95−104.

(36) Sheen, S.; Raptis, A. Acoustic flow instruments for solid/gas flow. *Part. Sci. Technol.* **1987**, *5*, 219−234.

(37) Pandey, P. M.S. Thesis, West Virginia University, Morgantown, WV, 2002.

(38) Bi, H.; Grace, J. Flow regime diagrams for gas−solid fluidization and upward transport. *Int. J. Multiphase Flow* **1995**, *21* (6), 1229−1236.

(39) Rhodes, M.; Mineo, H.; Hirama, T. Particle motion at the wall of a circulating fluidized bed. *Powder Technol.* **1992**, *70*, 207−214.

(40) Harris, A.; Davidson, J.; Thorpe, R. The prediction of particle cluster properties in the near wall region of a vertical riser. *Powder Technol.* **2002**, *127*, 128−143.

(41) Hatano, H.; Takeuchi, H.; Masuyama, T.; Tsuchiya, K. Motion of individual FCC particles and swarms in a circulating fluidized bed riser analyzed via high-speed imaging. *AIChE Symp. Ser.* **1998**, No. 318, *94*, 31−36.

(42) Glicksman, L. In *Circulating Fluidized Beds*; Grace, J., Avidan, A., Knowlton, T., Eds.; Blackie Academic and Professional: London, 1997; pp 261−311.

(43) Griffith, A.; Louge, M. The scaling of cluster velocity at the wall of circulating fluidized bed risers. *Chem. Eng. Sci.* **1998**, *53* (13), 2475−2477.

(44) Soong, C.; Tuzla, K.; Chen, J. Experimental determination of cluster size and velocity in circulating fluidized bed. In *Proceedings of the 8th Engineering Foundation Conference on Fluidization*; Large, J., Laguerie, C., Eds.; Engineering Foundation: New York, 1995; pp 219−227.

(45) Sharma, A.; Kemal, T.; Matsen, J.; Chen, J. Parametric effects of particle size and gas velocity on cluster characteristics in fast fluidized beds. *Powder Technol.* **2000**, *111*, 114−122.

(46) Zhang, W.; Tung, Y.; Johnson, F. Radial voidage profiles in fast fluidized beds of different diameters. *Chem. Eng. Sci.* **1991**, *46* (12), 3045−3052.

(47) Noymer, P.; Glicksman, L. Descent velocities of particle clusters at the wall of a circulating fluidized bed. *Chem. Eng. Sci.* **2000**, *55*, 5283−5289.

(48) Gidaspow, D.; Tsuo, Y.; Luo, K. Computed and experimental cluster formulation and velocity profiles in circulating fluidized beds. In *Fluidization VI*; Grace, J., Shemitt, L., Bergougnou, M., Eds.; Engineering Foundation: New York, 1989; pp 81−88.

(49) Lim, K.; Zhou, J.; Finley, C.; Grace, J.; Lim, C.; Brereton, C. Cluster descending velocity at wall of circulating fluidized bed risers. In *Proceedings of the 5th International Conference on Circulating Fluidized Beds*; Kwauk, M., Li, Y., Eds.; Science Press: Beijing, China, 1996; pp 218−223.

(50) Lints, M.; Glicksman, L. The structure of particle clusters near the wall of a circulating fluidized bed. *AIChE Symp. Ser.* **1993**, *89* (296), 35−52.

(51) Wirth, K.; Seiter, M.; Molerus, O. Concentration and velocities of solids in areas close to the walls in circulating fluidized beds systems. *VGB Kraftwerkstech.* **1991**, *10*, 824−828.

(52) Tsukada, M.; Ito, M.; Kamiya, H.; Horio, M. Three-dimension imaging of particle clusters in dilute gas−solid suspension flow. *Can. J. Chem. Eng.* **1997**, *75*, 466−470.

(53) Ishii, H.; Nakajima, T.; Horio, M. The clustering annular flow model of circulating fluidized beds. *J. Chem. Eng. Jpn.* **1989**, *22* (5), 484−490.

(54) Subbarao, D. Clusters and lean-phase behavior. *Powder Technol.* **1986**, *46*, 101−107.

(55) Moortel, T.; Tadrist, L. Flow structures in a circulating fluidized bed. In *Circulating Fluidized Bed Technology VII*; Grace, J., Zhu, J., de Lasa, H., Eds.; Canadian Society of Chemical Engineering: Ontario, Canada, 2002; pp 217−224.

(56) Yerushalmi, J.; Cankurt, N.; Geldart, D.; Liss, B. Flow regimes in vertical gas−solid contact systems. *AIChE Symp. Ser.* **1976**, *74* (176), 1−13.

(57) Monazum, E.; Shadle, L.; Lawson, L. A transient method for determination of saturation carrying capacity. *Powder Technol.* **2001**, *121*, 205−212.

(58) Ludlow, C.; Shadle, L.; Syamlal, M. Development of Spiral Device for Measuring Solids Flow. In *Circulating Fluidized Bed Technology VII*; Grace, J., Zhu, J., de Lasa, H., Eds.; Canadian Society of Chemical Engineering: Ontario, Canada, 2002; pp 513−520.

(59) Haider, A.; Levenspiel, O. Drag coefficient and terminal velocity of spherical and nonspherical particles. *Powder Technol.* **1989**, *58*, 63−70.

(60) Shadle, L.; Monazum, E.; Mei, J. Circulating fluid bed operating regimes. In *Circulating Fluidized Bed Technology VII*; Grace, J., Zhu, J., de Lasa, H., Eds.; Canadian Society of Chemical Engineering: Ontario, Canada, 2002; pp 255−262.

(61) Li, Y.; Kwauk, M. The dynamics of fast fluidization. In *Fluidization*; Grace, J., Matsen, J., Eds.; Plenum Press: New York, 1980; pp 537−544.

(62) Tadrist, L.; Cattiew, P. Analysis of two-phase flow in a circulating fluidized bed. In *Proceedings of the 4th International Conference on Circulating Fluidized Beds*; Avidan, A. A., Ed.; Mobil Research and Development Corp.: Paulsboro, New Jersey, 1993; pp 702−707.

(63) Karri, S.; Knowlton, T. Wall solids upflow and downflow regimes in risers for Group A solids. In *Circulating Fluidized Bed Technology VII*; Grace, J., Zhu, J., de Lasa, H., Eds.; Canadian Society of Chemical Engineering: Ontario, Canada, 2002; pp 310−316.

(64) Lints, M. Doctoral Thesis, Massachusetts Institute of Technology, Cambridge, MA, 1992.

(65) Wu, R.; Grace, J.; Lim, C. A model for heat transfer in circulating fluidized beds. *Chem. Eng. Sci.* **1990**, *45* (12), 3389−3398.